



# Characteristics of cellulose microfibers and nanocrystals isolated from doum tree (*Chamaerops humilis* var. *argentea*)

Adil Bahloul · Zineb Kassab · Faissal Aziz · Hassan Hannache · Rachid Bouhfid · Abou El Kacem Qaiss · Mina Oumam · Mounir El Achaby

Received: 17 September 2020 / Accepted: 22 February 2021 / Published online: 5 March 2021  
© The Author(s), under exclusive licence to Springer Nature B.V. 2021

**Abstract** Doum is a type of palm tree having leaves with a lower surface (looking like palm leaves) and trunk with relatively reduced height (< 1 m). It is naturally growing in a wide range of conditions and tolerating extreme temperatures (36–38 °C). In this work, doum leaves fibers and doum trunk fibers were identified as potential sources to produce cellulose derivatives, namely cellulose microfibers (CMFs) and cellulose nanocrystals (CNCs). CMFs were obtained from the identified sources via chemical treatments and then subjected to sulfuric acid hydrolysis to produce CNCs. The studied materials were characterized at different stages of treatment. It was found that CMFs, extracted from both sources, exhibited a

uniform size with a microfiber diameter ranged from 3 to 10 µm and crystallinity between 80 and 76%. The as-produced CNCs showed the same characteristics with an average diameter of 5.3 nm, an average length of about 450 nm and a crystallinity of 90%. This study can draw the attention of researchers towards doum tree as a new source of cellulosic materials. Owing to their excellent characteristics, the produced CMFs and CNCs could be used as additives or reinforcing agents for polymer composite development and beyond.

**Keywords** Doum tree · Cellulose microfibers · Cellulose nanocrystals · Acid hydrolysis

---

A. Bahloul · H. Hannache · M. Oumam  
Laboratoire d'Ingénierie et Matériaux (LIMAT), Faculté des Sciences Ben M'sik, Université Hassan II de Casablanca, B.P. 7955, Casablanca, Morocco

Z. Kassab (✉) · H. Hannache · M. El Achaby (✉)  
Materials Science and Nano-Engineering (MSN)  
Department, Mohammed VI Polytechnic University (UM6P), Lot 660 – Hay Moulay Rachid, 43150 Ben Guerir, Morocco  
e-mail: zineb.kassab@um6p.ma

M. El Achaby  
e-mail: mounir.elachaby@um6p.ma

F. Aziz  
National Centre for Research and Study on Water and Energy (CNEREE), Cadi Ayyad University, Marrakech, Morocco

R. Bouhfid · A. E. K. Qaiss  
Composites and Nanocomposites Center (CNC), Moroccan Foundation for Advanced Science, Innovation and Research (MAScIR), Rabat Design Center, Rue Mohamed El Jazouli, Madinat El Irfane, 10100 Rabat, Morocco

## Introduction

Recently, cellulosic fibers have captured more research attention in many engineering fields due to their interesting features, such as biocompatibility, biodegradability, renewability, low-cost, and non-toxicity (Camarero Espinosa et al. 2013). Cellulosic fibers have excellent properties such as lower density, good mechanical properties, and adaptable surface characteristics (Rajinipriya et al. 2018). They have become one of the essential bio-resourced materials that can be used in a wide range of advanced applications such as paper, textiles, composites, water purification, food packaging, cosmetic, and pharmaceutical industries (Rajinipriya et al. 2018; Kumar et al. 2020). However, with increasing demand for cellulose-based materials, as well as the need of new sources for the production of cellulose, pushed scientists and researchers to seek alternatives to wood, cotton, hemp, flax, and jute, which are the main conventional sources for the production of cellulose derivatives (Rajinipriya et al. 2018; Kumar et al. 2020). In this way, identifying new renewable sources for cellulose production has steadily increased recently (Prasad Reddy and Rhim 2014; Frone et al. 2017). In this context, various non-woody resources such as agricultural residues (wheat and maize straw, sugarcane bagasse, coconut husk and banana pseudostem fibers), fruit and vegetable wastes (tomato peel, banana peel, pineapple leaves and grape skins), agro-industrial residues (birch veneer and sawdust), perennial plants residues (mengkuang leaves, mulberry bark and sisal leave fibres), stem (bast) fibres (kenaf and ramie among others), grasses (bamboo, fodder grass and alfa) and waste papers (old newspapers, office waste papers and old corrugated containers) have been recently identified as renewable sources for cellulose derivatives production (Kumar et al. 2020). Cellulose can also be obtained from some other small class of sources like marine animals (tunicate), marine biomass (algae), fungi and bacteria (Rajinipriya et al. 2018). However, various unexplored valuable cellulose-rich materials were found in nature and that are not yet valorized for the production of cellulose derivatives.

Doum tree (*Chamaerops humilis* var. *argentea*), is a type of palm tree belonging to the Arecaceae family, having leaves (looking like the palm leaves) and trunk with relatively reduced height (< 1 m) (Jawaid et al.

2017). It is the only palm species naturally distributed in both Europe and Africa, it can be found in the western Mediterranean basin, especially in Italy, Sardinia, Spain, Libya, Tunisia, Algeria and Morocco (Fardioui et al. 2016; Guzmán et al. 2017; Mokbli et al. 2018). It is naturally growing in a wide range of conditions, tolerating extreme temperatures and conditions of the Mediterranean ecosystems (Mokbli et al. 2018). Fibers from doum tree were traditionally used to produce canvas, mats, baskets and ropes (Fardioui et al. 2016). Due to the high amount of cellulose, they can be used as a source of cellulose derivatives, such as micro- and nano-sized cellulose fibers.

Because of the biodiversity of cellulose sources, source components have a wide range of chemical compositions, i.e., cellulose, hemicelluloses, and lignin, and various cellulose forms with different morphologies, structures, and properties can be obtained. Purified cellulose microfibrils (CMFs) can be produced from cellulose-rich renewable sources using chemical methods such as alkalization and bleaching treatments (Sharma et al. 2019; Kassab et al. 2020a). CMFs consist of a mixture of amorphous and crystalline regions and exhibit a fiber diameter generally of several micrometers (Sharma et al. 2019). Once CMFs are produced, cellulosic polymers such as hydroxyethyl cellulose, ethyl cellulose, hydroxypropyl cellulose, cellulose acetate, cellulose nitrate, carboxymethyl cellulose and others could be obtained, through etherification, esterification, oxidation and nitration reactions. Most importantly, CMF can be converted into nanocellulose structures such as cellulose nanocrystals (CNCs) and cellulose nanofibrils (CNFs) by top-down procedures very unique to its own structure, such as acid hydrolysis or mechanical treatment (ultrasonic cell crusher, high shear homogenizer and centrifugation) (Du et al. 2020; Kassab et al. 2020e). Hence, the various forms of nanocellulose (CNCs, CNFs) and other forms (such as cellulose nanospheres) are expected to bring new life into cellulose next to conventional utilization of cellulose in the form of macro- and micro-fibers and derivatized polymers.

Nanostructured CNCs can be extracted from purified CMFs, using several methods such as mechanical, chemical and biological treatments (Kargarzadeh et al. 2017; Kassab et al. 2020e). Among these methods, the chemical treatment by mineral acid hydrolysis is the most used method (Camarero Espinosa et al. 2013;

Youssef et al. 2015). The conditions of acid hydrolysis, including cellulose source, type of acid and concentration, reaction temperature and duration, largely affect the characteristics the obtained CNCs (Kassab et al. 2020c). A variety of mineral acids have been used to extract CNCs, including phosphoric, sulfuric, hydrochloric and a mixture of acids. Sulfuric acid hydrolysis is the most commonly used for CNC extraction; it generates CNCs with embedded sulfate groups on the surface and providing high colloidal dispersibility and relatively low thermal stability to CNCs (Kassab et al. 2020c). On the other side, phosphoric acid hydrolysis creates phosphorylated CNCs with surface inserted phosphate groups, typically low in colloidal dispersibility but high in thermal stability (Camarero Espinosa et al. 2013).

To the best of authors' knowledge, no systematic research data regarding the extraction, characterization and comparison of cellulose derivatives from doum leaves and trunk fibers have been reported in the literature. Thus, to fulfil the research gap, the objectives of this study is to investigate the extraction and characterization of cellulose microfibrils (CMFs) and cellulose nanocrystals (CNCs) from the largely available Moroccan doum leaves and trunk fibers, as potential natural sources to produce cellulose derivatives (CMFs and CNCs). The physico-chemical properties of the as-extracted CMFs and CNCs were characterized using scanning electron microscopy (SEM), atomic force microscopy (AFM), infrared spectroscopy (FTIR), X-ray diffraction (XRD) and thermogravimetric analysis (TGA).

## Materials and methods

### Materials

DLF and DTF raw materials used during this work were harvested from the Doum tree, which are widespread along the banks of Nfifikh River (Casablanca-Settat region, Morocco). The collected products were firstly dried at 60 °C for 48 h and then ground using a precision grinder (Retch SM100) equipped with a 1 mm sieve. Analytical grade chemicals, such as sodium hydroxide, sodium chlorite, acetic acid and sulfuric acid, were purchased from Sigma-Aldrich and used as received.

### Extraction of cellulose microfibrils

Purified cellulose microfibrils (CMFs) were produced from DLF and DTF sources using the same extraction process, according to our previous works (Kassab et al. 2020a, c). Briefly, the ground fibers were firstly immersed in hot distilled water (60 °C) for 1 h to remove foreign particle, dust and water-soluble parts. Afterward, the washed fibers were alkali-treated using a 4 wt.% sodium hydroxide (NaOH) solution. Then, the obtained alkali-treated fibers were subjected to bleaching treatment, which was carried out using a bleaching solution made up of equal parts (v:v) of acetate buffer (27 g NaOH and 75 mL glacial acetic acid, diluted to 1 L of distilled water) and aqueous sodium chlorite (1.7 wt% NaClO<sub>2</sub> in water). For both alkali and bleaching treatments were done three times under mechanical stirring for 2 h at 80 °C, and the ratio of the fibers to liquor was fixed at 1/20 (g/mL). These treatments resulted in pure white-colored cellulose microfibrils, which were coded as CMF<sub>DLF</sub> and CMF<sub>DTF</sub> (Fig. 1), for the cellulose extracted from DLT and DTF sources, respectively.

### Extraction of cellulose nanocrystals

Cellulose nanocrystals (CNCs) were extracted by subjecting the as-extracted CMF<sub>DLF</sub> and CMF<sub>DTF</sub> to sulfuric acid hydrolysis, according to our previous works (Kassab et al. 2020a, b). In this process, never dried CMF<sub>DLF</sub> or CMF<sub>DTF</sub> were introduced into a preheated sulfuric acid solution (64 wt%) at 50 °C under mechanical stirring for 30 min. Then, the mixture was diluted with ice cubes to stop the reaction. The obtained mixture was washed several times with distilled water by using successive centrifugations at 12,000 rpm for 15 min at 15 °C for each time (Ultracentrifuge 100NX, himac CP-NX series, HITACHI). This washing process resulted in purely white CNC mixtures, which were subjected to dialysis step against distilled water until reaching a neutral pH. The as-produced CNC mixtures were then homogenized by using a probe-type ultrasonic homogenizer (BRANSON, Sonifier 250) for 5 min in an ice bath, resulting in white gel suspension (Fig. 2a, c). Finally, a quantity of the homogenized suspensions was freeze-dried to obtain the CNCs in solid form, resulting in a foam-like structure, as shown in Fig. 2b, d. During this work, the extracted CNCs were coded as CNC<sub>DLF</sub> and

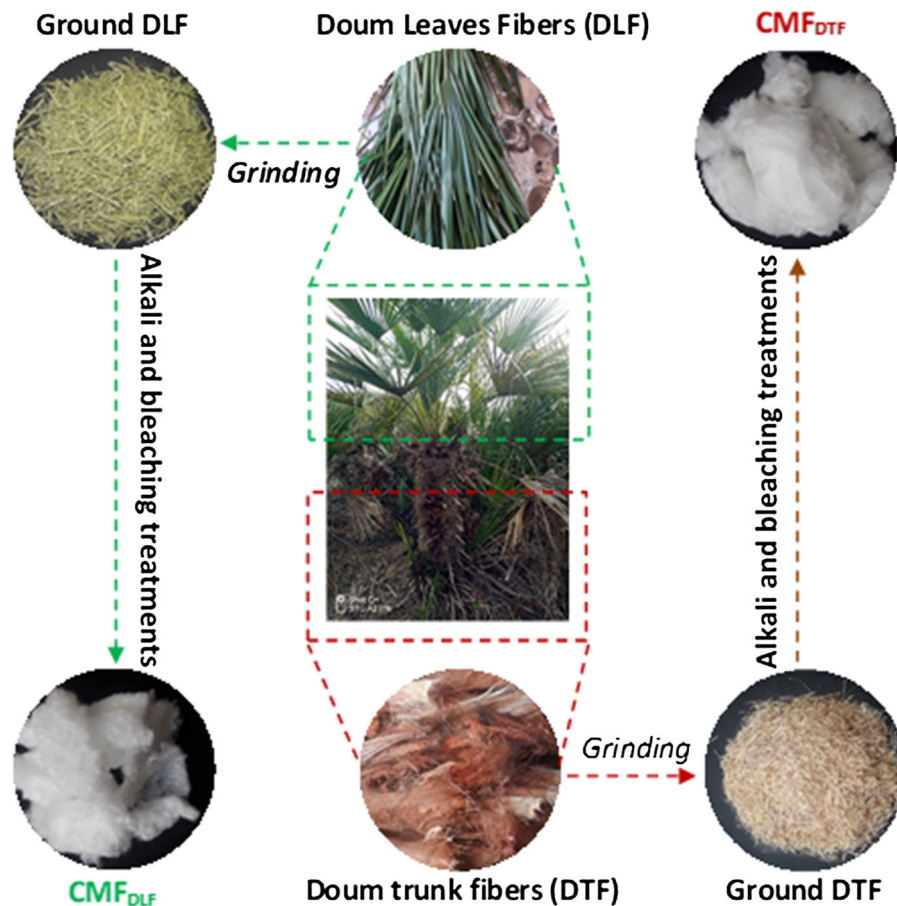


**Fig. 1** Extraction process of CMFs (CMF<sub>DLF</sub> and CMF<sub>DTF</sub>) from the selected two parts (DLF and DTF) of the Doum tree

CNC<sub>DTF</sub> for CNCs extracted from DLF and DTF sources, respectively.

#### Characterization techniques

The chemical composition of R-EPR was analyzed using TAPPI (Technical Association of the Pulp and Paper Associations) standard methods, according to our previous work (Bahloul et al. 2021). The morphology of the produced CMFs (CMF<sub>DLF</sub> and CMF<sub>DTF</sub>) was evaluated by using scanning electron microscopy (HIROX SH 4000 M) operated at 20 kV. The samples were first coated by a thin conductive carbon layer to help improve SEM images. The shapes and dimensions of the as-produced CNCs (CNC<sub>DLF</sub> and CNC<sub>DTF</sub>) were studied by using Atomic force microscopy (AFM) (Dimension ICON, Bruker). Samples for AFM observations were prepared by depositing droplets of diluted CNC suspensions (0.01 wt%)

onto freshly cleaved mica sheets, after being sonicated for 5 min and allowing the solvent to dry in air. The obtained AFM images and the dimensions of CNCs were analysed using Veeco data processing software (Nanoscope Version 8.0).

The chemical structures of all studied samples were evaluated by Fourier Transform Infrared Spectroscopy (FTIR) (Perkin-Elmer Spectrum 2000) equipped with ATR accessory. The experiments were recorded in transmittance mode in the range of 4000–400 cm<sup>-1</sup> with a resolution of 4 cm<sup>-1</sup> and an accumulation of 16 scans. The thermal stability and degradation behaviour of the studied cellulosic samples was conducted using thermogravimetric analysis (TGA) (Discovery TGA, TA Instrument). The analysis was performed under a nitrogen atmosphere between 25 and 700 °C, at a heating rate of 10 °C/min. The crystalline structure and crystallinity of the cellulosic samples were performed on an X-ray diffractometer (Bruker

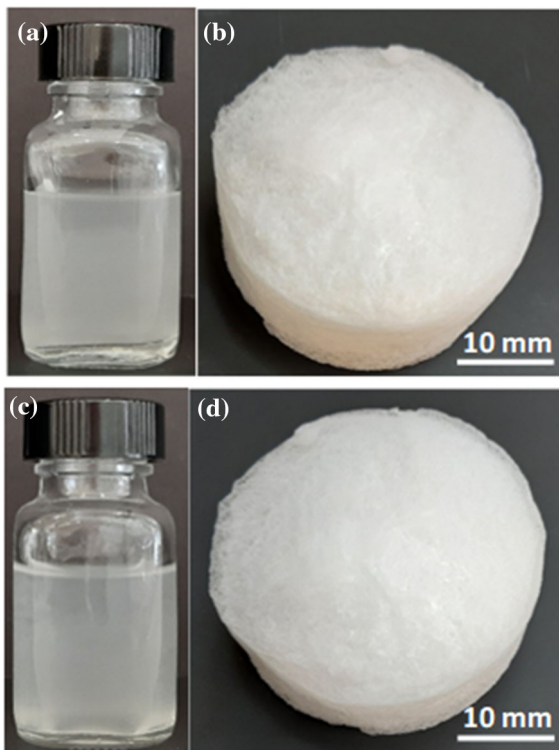


**Fig. 2** a Aqueous suspension of a  $\text{CNC}_{\text{DLF}}$  and c  $\text{CNC}_{\text{DTF}}$ , and foam-like structure of b  $\text{CNC}_{\text{DLF}}$  and d  $\text{CNC}_{\text{DTF}}$

diffractometer D8 Advance, Bruker). Samples were scanned with  $\text{CuK}$  radiation ( $\lambda = 1.54056 \text{ \AA}$ ) in the  $2\theta$  range of  $5\text{--}50^\circ \text{C}$ , while the voltage and current were fixed at 40 kV and 40 mA, respectively. The crystallinity index ( $\text{CrI}$ ) was calculated according to Segal equation:  $\text{CrI} = \frac{I_{200} - I_{\text{am}}}{I_{200}} \times 100$ , where  $I_{200}$  is the intensity of the 200-lattice plane at around  $2\theta = 22.8^\circ$ , and  $I_{\text{am}}$  is the intensity from the amorphous phase at approximately  $2\theta = 18.6^\circ$  (Kassab et al. 2020a).

## Results and discussions

### Chemical composition of raw fibers and morphology of CMFs

The chemical composition of the identified and studied DLF and DTF sources was determined, and the results are summarized in Table 1. These sources are considered as lignocellulosic fibers which are composed mainly of cellulose ( $\sim 29\text{--}30\%$ ), lignin

( $\sim 28\text{--}33\%$ ) and hemicelluloses ( $\sim 18\text{--}19\%$ ) components. The natural character and the renewability of these fibers make them excellent candidates for replacing synthetic fibers, especially for developing fibers-reinforced composite materials, thus pushing the research and development to move towards environmentally friendly materials. This interest is motivated by serious environmental concerns related not only to the unsustainable production processes of synthetic fibres, but also to the limited recyclability of synthetic fibers-reinforced composites and their end of life disposal options.

In this work, the identified cellulose-rich sources (DLF and DTF) were used for isolating cellulose microfibrils (CMFs) and nanocrystals (CNCs), using chemical routes. The first stage of treatment was focused on the isolation of single CMFs from DLF and DTF sources by applying alkali and bleaching treatments. These treatments are well-known processes applied to lignocellulosic fibers for their purification by removing of non-cellulosic components (Kassab et al. 2020a, e). Herein, we assumed that these applied treatments were effective for removing most of all non-cellulosic components such as hemicellulose and lignin molecules, resulting in purified cellulose fibers. It should be noted that the homogeneity, morphology and size of the lignocellulosic sources-derived cellulose fibers are strongly related to the source and the experimental conditions of alkali and bleaching treatments (concentration, reaction time and temperature) (Elseify et al. 2019). Herein, the applied chemical treatments to DLF and DTF sources resulted in the production of CMFs ( $\text{CMF}_{\text{DLF}}$  and  $\text{CMF}_{\text{DTF}}$ ) with good homogeneity, micrometric scale and smooth surface, as revealed by the SEM micrographs presented in Fig. 3. Noticeably,  $\text{CMF}_{\text{DLF}}$  and  $\text{CMF}_{\text{DTF}}$  showed almost the same microfiber diameter, which is ranged from 3 to  $10 \mu\text{m}$ , indicating that the two selected parts of the Doum tree exhibited the same cellulose fibers quality.

As summarized in Table 2, the obtained average diameter is smaller than that of CMF extracted from sisal, cotton, flax, sugar palm fibres, hemp and tomato plant residue. Contrastingly, it is higher than that of CMF extracted from softwood kraft pulp, juncus plant and pineapple leaf (Table 2). Consequently, the original DLF and DTF fibers can be classified as less common natural fibers. However, their physical aspect, chemical composition and characteristics are

**Table 1** Chemical composition of the studied raw DLF and DTF sources

Source	Cellulose (%)	Lignin (%)	Hemicelluloses (%)	Ash (%)	Moisture (%)
DLF	30.86	33.12	18.57	2.23	8.20
DTF	29.01	28.64	19.74	4.79	10.62

similar to the well-known fibers such as kenaf, hemp, sisal, flax and jute. The obtained CMFs from these newly identified sources exhibited a relatively small diameter, making them good candidates for developing advanced micro-cellulose-based materials. Besides, the obtained CMFs were suitable for nano-sized cellulose extraction using acid hydrolysis process. The role of acid hydrolysis is to dissolve the amorphous domains of the CMFs, producing CNCs with excellent characteristics.

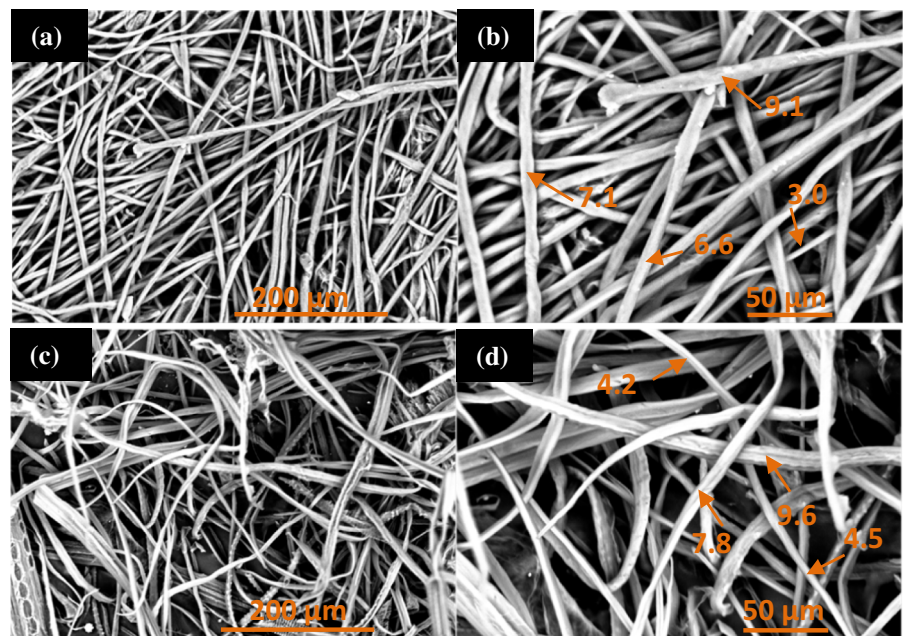
#### Morphology and dimensions of CNCs

CNCs were extracted from  $\text{CMF}_{\text{DLF}}$  and  $\text{CMF}_{\text{DTF}}$  being named  $\text{CNC}_{\text{DLF}}$  and  $\text{CNC}_{\text{DTF}}$ , respectively. AFM observations were carried out to confirm the extraction of CNCs and to evaluate their morphologies and dimensions at the nanometric scale. Figure 4a–d display AFM images of the as-developed  $\text{CNC}_{\text{DLF}}$  and  $\text{CNC}_{\text{DTF}}$ , respectively. It is worthy to note that the

nanostructures of cellulose were successfully isolated with well-defined needle-like shaped nanocrystal, confirming that the Doum tree-derived CMFs are suitable for CNC development. Herein, the treatment of CMFs by concentrated sulfuric acid resulted in transversely cleaving of the amorphous region of CMF, leaving the crystalline regions unaltered. Eventually, the size of the fibers was reduced from the micron to the nanometric scale (Grishkewich et al. 2017; Rajinipriya et al. 2018).

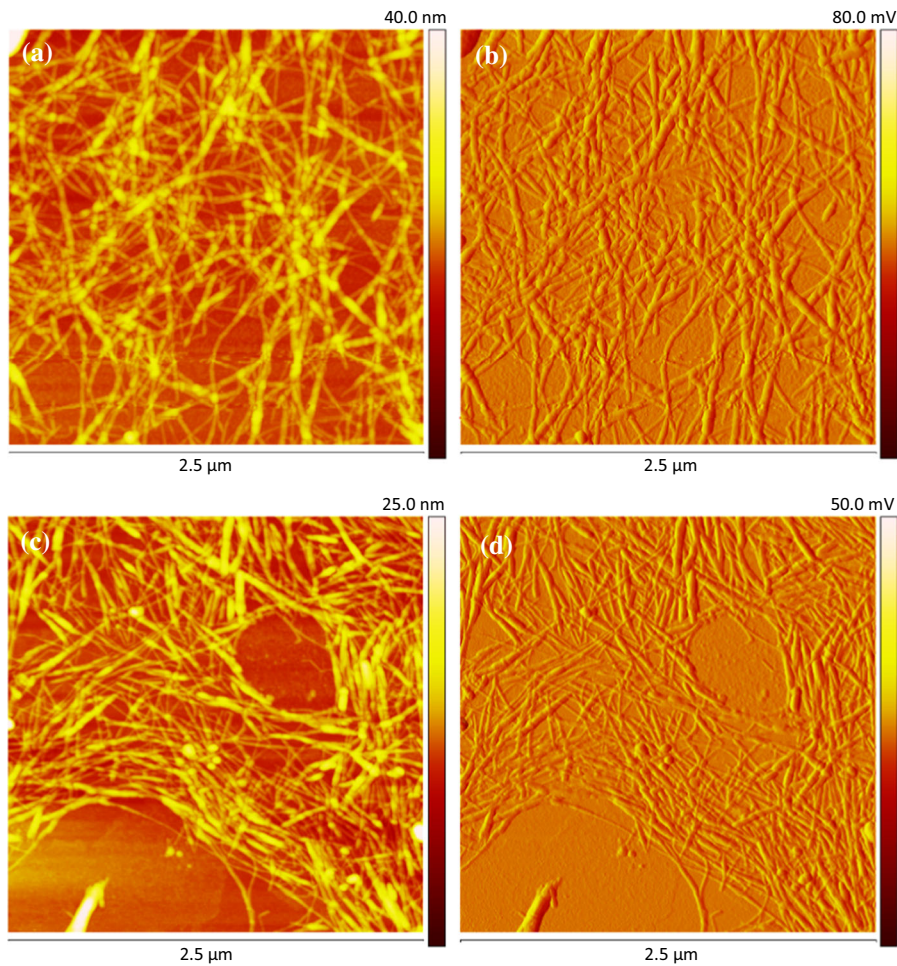
The treatment of AFM images revealed that the extracted CNCs exhibit a diameter ( $D$ ) of  $5.2 \pm 1.2$  nm and  $5.4 \pm 1.1$  nm, while the length ( $L$ ) was determined at  $435 \pm 98$  nm and  $467 \pm 86$  nm for  $\text{CNC}_{\text{DLF}}$  and  $\text{CNC}_{\text{DTF}}$ , respectively. Within the statistical error, both CNCs are characterized by almost the same dimensions in terms of  $D$  and  $L$ , indicating that the CMFs from the two selected parts of the Doum tree can be hydrolyzed in the same way when subjected to sulfuric acid treatment. The

**Fig. 3** SEM images of a, b  $\text{CMF}_{\text{DLF}}$  and c, d  $\text{CMF}_{\text{DTF}}$



**Table 2** Diameter of CMF extracted from various lignocellulosic fibers

Source	Diameter ( $\mu\text{m}$ )	References
Sisal	287	Ludueña et al. (2013)
Cotton	131	Ludueña et al. (2013)
Sugar palm fibres	122	Phuong et al. (2017)
Bamboo fibres	15	Rasheed et al. (2020)
Flax	51	Ludueña et al. (2013)
Hemp stalks	17	Kassab et al. (2020a)
Tomato plant residue	20	Kassab et al. (2020c)
Banana peel	19	Harini et al. (2018)
Bract	15	Harini et al. (2018)
Pineapple leaf	4	Fareez et al. (2018)
Juncus plant	3	Kassab et al. (2020d)
Softwood kraft pulp	0.1–1	Chakraborty et al. (2006)
DLF and DTF	3–10	This work

**Fig. 4** AFM images of **a, b** CNC<sub>DLF</sub> and **c, d** CNC<sub>DTF</sub> in height and amplitude mode

measured CNC dimensions are comparable to those determined for CNCs extracted from recently identified lignocellulosic sources (natural fibers, agricultural residues, marine algae) such as *Juncus* fibers ( $D = 7.3 \pm 2.2$  nm,  $L = 431 \pm 94$  nm) (Kassab et al. 2020e), oil palm trunk (*Elaeis guineensis*) ( $D = 7.67$  nm,  $L = 397.03$  nm) (Lamaming et al. 2015b), tomato plant residue ( $D = 7.4 \pm 2.2$  nm,  $L = 367 \pm 101$  nm) (Kassab et al. 2020c), tomato peels ( $D = 5\text{--}9$  nm,  $L = 100\text{--}200$  nm) (Jiang and Hsieh 2015). More importantly, the measured CNC diameters is closed to those obtained from the conventional sources of cellulose such as wood pulp ( $D = 3\text{--}8$  nm) (Lahiji et al. 2010), cotton ( $D = <10$  nm) (Hsieh 2013) and tunicin ( $D = 9.4 \pm 5.0$  nm) (Sacui et al. 2014). Owing to this, the Doum tree can be considered as a potential lignocellulosic source for the production of cellulosic nanomaterials with high quality, which can be used for many multifunctional applications, such as nanoadditives or nanoreinforcing agents for water-soluble polymers in order to produce bio-nanocomposites by solvent casting techniques (Kassab et al. 2020b).

#### Chemical structure of CMFs and CNCs

In order to determine the chemical structure, raw DLF and DTF, CMF<sub>DLF</sub> and CMF<sub>DTF</sub> and CNC<sub>DLF</sub> and CNC<sub>DTF</sub> samples were analyzed using FTIR-ATR spectroscopy as showed in Fig. 5. The raw DLF and DTF showed a band at  $1732\text{ cm}^{-1}$ , indicating the presence of the carbonyl function of acetyl groups of lignin and hemicellulose (Prasad Reddy and Rhim 2014; Ajouguim et al. 2019). While bands at  $1514$  and  $1460\text{ cm}^{-1}$  are attributed to C=C and C–C=C groups vibration stretching from aromatic hydrocarbons of lignin (Fardioui et al. 2016; Kassab et al. 2020e). The absorption band at  $1242\text{ cm}^{-1}$  is correlated to COO<sup>−</sup> groups of hemicelluloses (Prasad Reddy and Rhim 2014; Kassab et al. 2020e). These bands disappeared in the CMF spectra, indicating that most of all hemicelluloses and lignin molecules was removed after the applied alkali and bleaching treatments.

Comparing the FTIR spectra of raw DLF and DTF with that of CMF<sub>DLF</sub> and CMF<sub>DTF</sub>, the absorption peak at  $1641\text{ cm}^{-1}$  is correlated with the vibration binding of water molecules absorbed into cellulose fiber structure (Fardioui et al. 2016), bands at  $1426$  and  $1315\text{ cm}^{-1}$  corresponding to CH<sub>2</sub> symmetric bending

groups of cellulose. The bands between  $1163$  and  $899\text{ cm}^{-1}$  are correlated with the β-(1–4) glucosidic ether linkages and the β-glycosidic linkages, C–O–C glycosidic symmetric stretching, C–OH stretching vibration and C–O stretching and C–H rocking vibrations of cellulose indicating the presence cellulose structure (Prasad Reddy and Rhim 2014; Fardioui et al. 2016; Kassab et al. 2020d). On the other hand, by comparing the FTIR spectra of CMF<sub>DLF</sub> and CMF<sub>DTF</sub> with that of CNC<sub>DLF</sub> and CNC<sub>DTF</sub>, no difference in the bands was observed. The spectra at  $1208\text{ cm}^{-1}$  of both NC corresponds to S=O bonding generated from sulfuric acid hydrolysis, overlapped with cellulose molecule characteristics bands (Mendes et al. 2015; Wu et al. 2019; Kassab et al. 2019). Thereby, FTIR results indicated a considerable variation in the chemical structure of raw DLF and DTF after alkali and bleaching treatments resulting in pure CMFs. At the same time, the cellulose structure was maintained, indicating the conservation of the molecular structure of cellulose after chemical treatment (Fardioui et al. 2016).

#### Crystalline structure of CMFs and CNCs

The crystalline structure and crystallinity of the studied cellulosic materials were evaluated by XRD analysis, and the obtained results are illustrated in Fig. 6. Notably, all samples showed the typical cellulose *I* structure, which is characterized by the main crystalline peaks located at approximately  $15.1^\circ$ ,  $16.1^\circ$ ,  $22.3^\circ$  and  $34.7^\circ$ , corresponding to  $1\bar{1}0$ ,  $110$ ,  $200$  and  $004$  typical reflection planes (Nishiyama et al. 2012; French 2014). This finding is generally observed for natural lignocellulosic sources and its cellulosic derivatives (Nishiyama et al. 2012; French 2014; Ditzel et al. 2017). It is important to note that the magnitude of the observed crystalline peaks increased for CMF and CNC samples compared to the raw materials because of the removal of most of all amorphous non-cellulosic components (lignin and hemicellulose).

The crystallinity index (*CrI*) of the studied materials was determined using the Segal equation described above, and the obtained results are summarized in Table 3. The *CrI* of CMF samples was found to be 76 and 80% for CMF<sub>DTF</sub> and CMF<sub>DLF</sub>, which is higher than that measured for raw DTF (53%) and



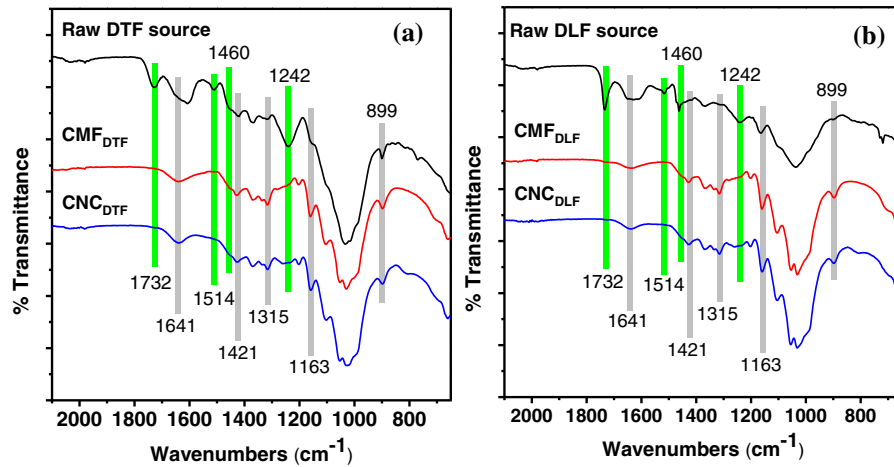


**Fig. 5** FTIR spectra of **a** raw DLF,  $\text{CMF}_{\text{DLF}}$  and  $\text{CNC}_{\text{DLF}}$ , **b** raw DTF,  $\text{CMF}_{\text{DTF}}$  and  $\text{CNC}_{\text{DTF}}$

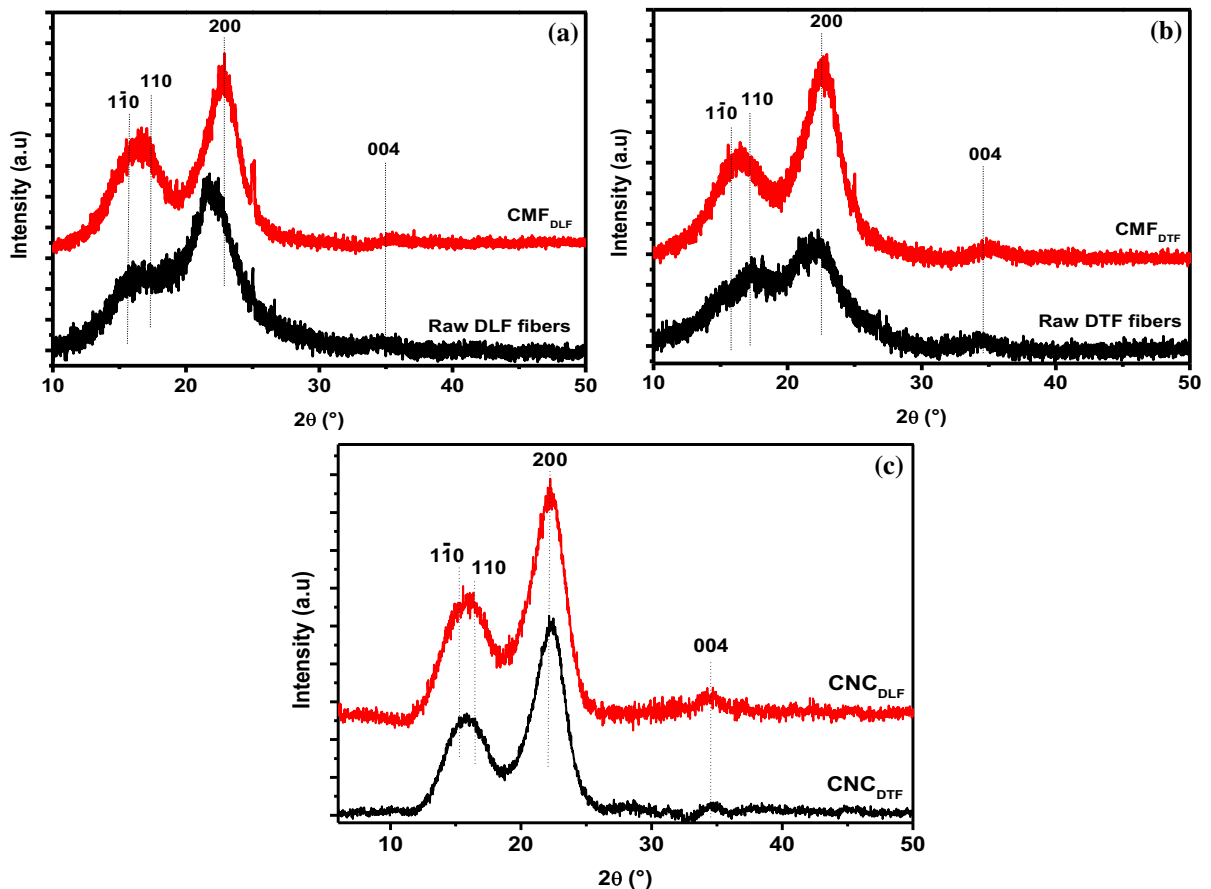


**Fig. 6** XRD patterns of **a** raw DLF and  $\text{CMF}_{\text{DLF}}$ , **b** raw DTF and  $\text{CMF}_{\text{DTF}}$ , **c**  $\text{CNC}_{\text{DLF}}$  and  $\text{CNC}_{\text{DTF}}$  samples

DLF (64%) sources. This is because of the presence of non-cellulosic components in raw sources, which are

totally removed after the applied chemical treatments. This result is in good accordance with SEM

observations that confirmed the production of single microfibers with a clean and smooth surface (Fig. 3). The determined  $CrI$  of CMF materials is comparable to that previously observed for commercial cellulose fibers (82.6%) (Yu et al. 2016).

By contrast, the extracted CNCs (CNC<sub>DTF</sub> and CNC<sub>DLF</sub>) showed narrowest and sharpest peaks due to their higher crystallinity regarding the raw and CMF samples. It was evaluated that CNCs exhibited a  $CrI$  of 91 and 89% for CNC<sub>DTF</sub> and CNC<sub>DLF</sub>, respectively. The higher  $CrI$  values of CNC samples compared to those of CMF samples is due to the hydrolysis of the amorphous regions of cellulose chains during the acid hydrolysis process (Kassab et al. 2020a). It has been reported that the growth and realignment of monocrytals may occur simultaneously during the acid hydrolysis of CMFs, hence producing CNCs with improved crystallinity (Meng et al. 2019). It is well-known that the rigidity, elasticity, strength and thermal stability of CNCs are proportional to their crystallinity (Lamaming et al. 2015a; Meng et al. 2019). Herein, the produced highly crystalline CNCs could be considered as good nanoreinforcing agents for polymer nanocomposite development.

#### Thermal stability of CMFs and CNCs

The thermal behaviour of the produced micro- (CMF<sub>DLF</sub> and CMF<sub>DTF</sub>) and nano-cellulosic (NC<sub>DLF</sub> and NC<sub>DTF</sub>), including raw materials (DLF and DTF), were evaluated by TGA/DTG analysis and the obtained results are shown in Fig. 7. It is worth noting that the lignocellulosic materials degrade at low to moderate temperatures. Their degradation starts at lower temperatures for hemicelluloses, followed by an

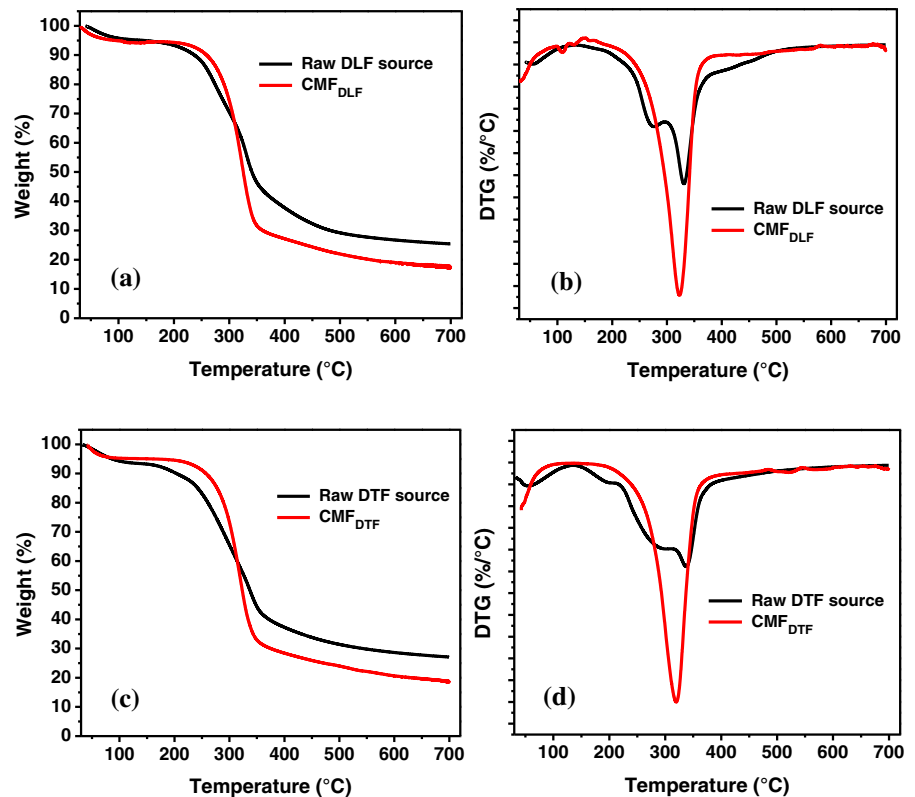
early stage of decomposition of lignin molecules and then degradation of cellulose (Kassab et al. 2020a). From Fig. 7, all samples showed a slight weight loss below 120 °C, which is due to the evaporation of water loosely bound to the surfaces of cellulose. The presence of water is attributed to the hydrophilic behaviour of these natural cellulosic materials (Luzi et al. 2019). Furthermore, raw DLF and DTF showed two steps decomposition process, as indicated by DTG curves (Fig. 7b). The onset temperature ( $T_{onset}$ ), the maximum degradation temperature ( $T_{max}$ ), and the char residue at 700 °C were determined and presented in Table 3. The  $T_{onset}$  of DLF and DTF was observed at 196 °C and 165 °C, respectively, with two maximum degradation temperatures ( $T_{max1}$  and  $T_{max2}$ ). The  $T_{max1}$  and  $T_{max2}$  were determined at 276 and 329 °C for the DLF and 281 and 337 °C for the DTF. Herein, the first degradation stage is associated with the decomposition of hemicellulose and lignin molecules, while the second one is attributed to the decomposition of cellulose molecules (Kassab et al. 2020a).

The purified CMFs (CMF<sub>DLF</sub> and CMF<sub>DTF</sub>) showed almost the same degradation behavior, which is processed in one step degradation process, confirming the removal of most of all lignin and hemicellulose molecules, which characterized by lower degradation temperatures, as observed in DLF and DTF samples. The samples CMF<sub>DLF</sub> and CMF<sub>DTF</sub> showed a  $T_{onset}$  of around 218 °C and 219 °C with a  $T_{max}$  of around 321 °C and 323 °C, respectively. Generally, the thermal decomposition of pure cellulose begins with the pyrolysis of glucose units followed by the depolymerization, dehydration processes and then completed by the oxidation and breakdown of the charred residue to lower molecular weight gaseous

**Table 3** Crystallinity index ( $CrI$ ) and thermal degradation parameters ( $T_{onset}$ ,  $T_{max}$  and char residue at 700 °C) of the studied samples

Sample	XRD analysis	TGA/DTG analysis			
	$CI$ (%)	$T_{onset}$ (°C)	$T_{max1}$ (°C)	$T_{max2}$ (°C)	Char residue (%) at 700 °C
DLF source	64	196	276	329	25
CMF <sub>DLF</sub>	80	218	–	321	18
CNC <sub>DLF</sub>	89	263	–	331	20
DTF source	53	165	281	337	27
CMF <sub>DTF</sub>	76	219	–	323	19
CNC <sub>DTF</sub>	91	265	–	323	22

**Fig. 7** TGA/DTG curves of **a, b** Raw DLF source and  $\text{CMF}_{\text{DLF}}$  and **c, d** Raw DTF source and  $\text{CMF}_{\text{DTF}}$  samples



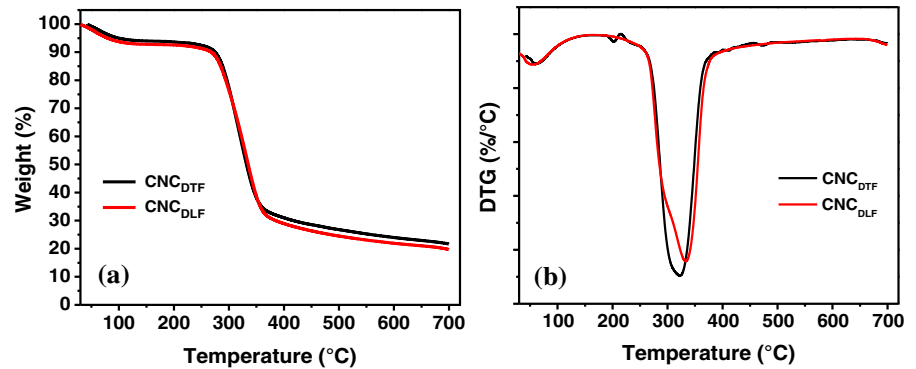
products (Meng et al. 2019). CMF samples are also characterized by lower char residue at 700 °C (18–19%) regarding the original DLF and DTF samples. The high char residues observed for DLF (25%) and DTF (27%) samples are due to the presence of hemicellulose and lignin molecules in these samples, which were removed after the applied alkali- and bleaching treatments, resulting in purified cellulose with high thermal stability and lower char residue.

Figure 8 shows the obtained TGA/DTG curves for the extracted CNCs. In general, sulfuric acid hydrolyzed CNCs are characterized by lower thermal stability, limiting their processing at relatively high temperatures. This is due to the presence of sulfate groups on the surface of CNCs inserted during the sulfuric acid hydrolysis process. It has been reported that the inserted sulfate groups on the surface of CNCs are capable of altering the thermal stability of CNCs because the activation energy is smaller with a higher amount of sulfate groups, thus suggesting a catalytic action on the effect of degradation reactions (Hafemann et al. 2019). Importantly, the thermal stability of CNCs is a key factor in order for them to be used as

effective nanoreinforcing materials for thermoplastics polymers having typical processing temperatures of above 200 °C.

In this work, the extracted  $\text{CNC}_{\text{DLF}}$  and  $\text{CNC}_{\text{DTF}}$  from Doum tree parts displayed a  $T_{\text{onset}}$  of around 263 °C and 265 °C with  $T_{\text{max}}$  of around 331 °C and 323 °C, respectively. Interestingly, the here obtained  $T_{\text{onset}}$  of the as-extracted CNCs is higher than that observed for sulfuric acid hydrolyzed CNCs extracted from various other sources using the same extraction conditions. A direct comparison of this finding is summarized in Table 4, in which the  $T_{\text{onset}}$  of the CNCs samples extracted in this work is compared with data from earlier published works for CNCs extracted from other sources. From Table 4, it can be seen that the  $T_{\text{onset}}$  is ranged from 130° to more than 270 °C, depending on the experimental conditions of sulfuric acid hydrolysis process (acid concentration, temperature and time of reaction), and also to the source of native cellulose used for CNC isolation. From this comparison, it can be concluded that the CNCs developed in work exhibited high thermal stability compared to that determined for CNCs from other

**Fig. 8** **a** TGA and **b** DTG curves of CNC<sub>DLF</sub> and CNC<sub>DTF</sub> samples



sources, suggesting that the native celluloses (CMFs) extracted from the Doum tree-derived sources (DLF and DTF) are suitable for extracting thermally stable CNCs by sulfuric acid, which represents the effective acid generally used for this purpose.

Moreover, CNCs (CNC<sub>DLF</sub> and CNC<sub>DTF</sub>) showed a char residue of around 20–22% (Table 3), which is slightly higher than that observed for CMFs samples

(18–19%), due to the insertion of sulfate groups on the surface of CNCs, acting as flame-retardants (Silvério et al. 2013; Kusmono et al. 2020). The same trend was previously observed for CNCs extracted from other sources using sulfuric acid hydrolysis process (Silvério et al. 2013; Oun and Rhim 2016; Luzi et al. 2019; Kusmono et al. 2020).

**Table 4** The onset temperature ( $T_{onset}$ ) of thermal degradation of CNCs extracted from various sources

Source	Experimental conditions <sup>a</sup> of sulfuric acid hydrolysis	$T_{onset}$ (°C)	References
Cotton (Whatman filter paper)	64%, 45 °C, 60 min	150	Camarero Espinosa et al. (2013)
Cotton fibers	60%, 45 °C, 30 min	205	Ludueña et al. (2013)
Sisal fibers	60%, 45 °C, 30 min	240	Ludueña et al. (2013)
Flax fibers	60%, 45 °C, 30 min	241	Ludueña et al. (2013)
Corn stover	60%, 45 °C, 30 min	238	Ludueña et al. (2013)
Rice husk	60%, 45 °C, 30 min	220	Ludueña et al. (2013)
Liquefied banana pseudo-stem residue	64%, 50 °C, 30 min	265	Meng et al. (2019)
Hemp stalks	64%, 50 °C, 30 min	177	Kassab et al. (2020a)
Tomato plant residue	64%, 50 °C, 30 min	219	Kassab et al. (2020c)
Corn cob	9.17 M, 45 °C, 30 min	200	Silvério et al. (2013)
Alfa fibers	64%, 50 °C, 30 min	170	El Achaby et al. (2018)
Juncus plant	64%, 50 °C, 30 min	221	Kassab et al. (2020e)
Ramie fibers	58%, 55 °C, 30 min	215	Kusmono et al. (2020)
Bamboo fibres	64%, 45 °C, 45 min	272	Rasheed et al. (2020)
Royal palm tree	64%, 35–45 °C, 10–40 min	130	Hafemann et al. (2019)
Oil palm trunk	64%, 45 °C, 60 min	165	Lamaming et al. (2015b)
Doum leaves fibers	64%, 50 °C, 30 min	263	This work
Doum trunk fibers		265	

<sup>a</sup>Acid concentration (%), Temperature (°C) and time (min)

## Conclusions

The successful isolation of cellulose microfibrils (CMFs) and cellulose nanocrystals (CNCs) from two main parts of the doum tree, namely leaves fibers (DLF) and trunk fibers (DTF), was realized for the first time in this work. The obtained CMFs (CMF<sub>DLF</sub> and CMF<sub>DTF</sub>) from these newly identified sources exhibited a relatively small diameter (3–10 μm) and high crystallinity (76–80%), which are better than those extracted from various well-known sources, making them good candidates for developing advanced micro-cellulose-based materials. By subjecting CMF<sub>DLF</sub> and CMF<sub>DTF</sub> to sulfuric acid hydrolysis, CNCs were separately obtained with different morphological characteristics. The produced CNC<sub>DLF</sub> and CNC<sub>DTF</sub> exhibited a needle-like shape with an average diameter of  $5.2 \pm 1.2$  and  $5.4 \pm 1.1$  nm, and an average length of  $435 \pm 98$  and  $467 \pm 86$  nm, while the crystallinity index was determined at 89 and 91%, respectively. The thermal stability of the extracted CNC<sub>DLF</sub> and CNC<sub>DTF</sub> was significantly higher than that reported in previous studies for CNCs isolated from other sources. These findings demonstrated a potential strategy to add value to the doum tree (leaves and trunk), rich in cellulose, inexpensive, largely abundant and underutilized renewable sources. The extracted CNC<sub>DLF</sub> and CNC<sub>DTF</sub> from the doum tree parts exhibited excellent characteristics, making them good candidates for multifunctional applications such as nanoreinforcing agents for polymer nanocomposites manufacturing.

**Acknowledgments** The financial assistance of the materials science and nanoengineering (MSN) Department of the Mohammed VI Polytechnic University (UM6P), toward this research is hereby acknowledged.

## Declarations

**Conflict of interest** The authors declare that they have no conflict of interest.

**Ethical approval** The article does not include human participants and/or animals research.

**Informed consent** Informed consent was obtained from all participants.

## References

- Ajouguim S, Abdelouahdi K, Waqif M et al (2019) Modifications of Alfa fibers by alkali and hydrothermal treatment. *Cellulose* 26:1503–1516. <https://doi.org/10.1007/s10570-018-2181-9>
- Bahloul A, Kassab Z, El Bouchti M et al (2021) Micro- and nano-structures of cellulose from eggplant plant (*Solanum melongena* L.) agricultural residue. *Carbohydr Polym* 253:117311. <https://doi.org/10.1016/j.carbpol.2020.117311>
- Camarero Espinosa S, Kuhnt T, Foster EJ, Weder C (2013) Isolation of thermally stable cellulose nanocrystals by phosphoric acid hydrolysis. *Biomacromolecules* 14:1223–1230. <https://doi.org/10.1021/bm400219u>
- Chakraborty A, Sain M, Kortschot M (2006) Reinforcing potential of wood pulp-derived microfibrils in a PVA matrix. *Holzforschung* 60:53–58. <https://doi.org/10.1515/HF.2006.010>
- Ditzel FI, Prestes E, Carvalho BM et al (2017) Nanocrystalline cellulose extracted from pine wood and corncob. *Carbohydr Polym* 157:1577–1585. <https://doi.org/10.1016/j.carbpol.2016.11.036>
- Du H, Parit M, Wu M et al (2020) Sustainable valorization of paper mill sludge into cellulose nanofibrils and cellulose nanopaper. *J Hazard Mater* 400:123106. <https://doi.org/10.1016/j.jhazmat.2020.123106>
- El Achaby M, Kassab Z, Barakat A, Aboulkas A (2018) Alfa fibers as viable sustainable source for cellulose nanocrystals extraction: application for improving the tensile properties of biopolymer nanocomposite films. *Ind Crops Prod* 112:499–510. <https://doi.org/10.1016/j.indcrop.2017.12.049>
- Elseify LA, Midani M, Shihata LA, El-Mously H (2019) Review on cellulosic fibers extracted from date palms (*Phoenix dactylifera* L.) and their applications. *Cellulose* 26:2209–2232. <https://doi.org/10.1007/s10570-019-02259-6>
- Fardioui M, Stambouli A, Gueddira T et al (2016) Extraction and characterization of nanocrystalline cellulose from doum (*Chamaerops humilis*) leaves: a potential reinforcing biomaterial. *J Polym Environ* 24:356–362. <https://doi.org/10.1007/s10924-016-0784-5>
- Fareez IM, Ibrahim NA, Wan Yaacob WMH et al (2018) Characteristics of cellulose extracted from Jospine pineapple leaf fibre after alkali treatment followed by extensive bleaching. *Cellulose* 25:4407–4421. <https://doi.org/10.1007/s10570-018-1878-0>
- French AD (2014) Idealized powder diffraction patterns for cellulose polymorphs. *Cellulose* 21:885–896. <https://doi.org/10.1007/s10570-013-0030-4>
- Frone AN, Chiulan I, Panaitescu DM et al (2017) Isolation of cellulose nanocrystals from plum seed shells, structural and morphological characterization. *Mater Lett* 194:160–163. <https://doi.org/10.1016/j.matlet.2017.02.051>
- Grishkewich N, Mohammed N, Tang J, Tam KC (2017) Recent advances in the application of cellulose nanocrystals. *Curr Opin Colloid Interface Sci* 29:32–45. <https://doi.org/10.1016/j.cocis.2017.01.005>

- Guzmán B, Fedriani JM, Delibes M, Vargas P (2017) The colonization history of the Mediterranean dwarf palm (*Chamaerops humilis* L., Palmae). *Tree Genet Genomes* 13:1–10. <https://doi.org/10.1007/s11295-017-1108-1>
- Hafemann E, Battisti R, Marangoni C, Machado RAF (2019) Valorization of royal palm tree agroindustrial waste by isolating cellulose nanocrystals. *Carbohydr Polym* 218:188–198. <https://doi.org/10.1016/j.carbpol.2019.04.086>
- Harini K, Ramya K, Sukumar M (2018) Extraction of nano cellulose fibers from the banana peel and bract for production of acetyl and lauroyl cellulose. *Carbohydr Polym* 201:329–339. <https://doi.org/10.1016/j.carbpol.2018.08.081>
- Hsieh LY (2013) Cellulose nanocrystals and self-assembled nanostructures from cotton, rice straw and grape skin: a source perspective. *J Mater Sci* 48:7837–7846. <https://doi.org/10.1007/s10853-013-7512-5>
- Jawaid M, Sapuan SM, Alotman OY (2017) Green biocomposites manufacturing and properties. *Green Biocompos.* <https://doi.org/10.1007/978-3-319-46610-1>
- Jiang F, Hsieh YL (2015) Cellulose nanocrystal isolation from tomato peels and assembled nanofibers. *Carbohydr Polym* 122:60–68. <https://doi.org/10.1016/j.carbpol.2014.12.064>
- Kargarzadeh H, Ioelovich M, Ahmad I et al (2017) Methods for extraction of nanocellulose from various sources. In: *Handbook of nanocellulose and cellulose nanocomposites*, pp 1–49. <https://doi.org/10.1002/9783527689972.ch1>
- Kassab Z, Boujemaoui A, Ben Youcef H et al (2019) Production of cellulose nanofibrils from alfa fibers and its nanoreinforcement potential in polymer nanocomposites. *Cellulose* 26:9567–9581. <https://doi.org/10.1007/s10570-019-02767-5>
- Kassab Z, Abdellaoui Y, Hamid Salim M, El Achaby M (2020a) Cellulosic materials from Pea (*Pisum sativum*) and broad beans (*Vicia faba*) pods agro-industrial residues. *Mater Lett* 280:128539. <https://doi.org/10.1016/j.matlet.2020.128539>
- Kassab Z, Abdellaoui Y, Salim MH et al (2020b) Micro- and nano-celluloses derived from hemp stalks and their effect as polymer reinforcing materials. *Carbohydr Polym* 245:116506. <https://doi.org/10.1016/j.carbpol.2020.116506>
- Kassab Z, Kassem I, Hannache H et al (2020c) Tomato plant residue as new renewable source for cellulose production: extraction of cellulose nanocrystals with different surface functionalities. *Cellulose* 27:4287–4303. <https://doi.org/10.1007/s10570-020-03097-7>
- Kassab Z, Mansouri S, Tamraoui Y et al (2020d) Identifying Juncus plant as viable source for the production of micro- and nano-cellulose fibers: application for PVA composite materials development. *Ind Crops Prod* 144:112035. <https://doi.org/10.1016/j.indcrop.2019.112035>
- Kassab Z, Syafri E, Tamraoui Y et al (2020e) Characteristics of sulfated and carboxylated cellulose nanocrystals extracted from Juncus plant stems. *Int J Biol Macromol* 154:1419–1425. <https://doi.org/10.1016/j.ijbiomac.2019.11.023>
- Kumar V, Pathak P, Bhardwaj NK (2020) Waste paper: an underutilized but promising source for nanocellulose mining. *Waste Manag* 102:281–303. <https://doi.org/10.1016/j.wasman.2019.10.041>
- Kusmono LRF, Wildan MW, Ilman MN (2020) Preparation and characterization of cellulose nanocrystal extracted from ramie fibers by sulfuric acid hydrolysis. *Heliyon* 6:e05486. <https://doi.org/10.1016/j.heliyon.2020.e05486>
- Lahiji RR, Xu X, Reifengerger R et al (2010) Atomic force microscopy characterization of cellulose nanocrystals. *Langmuir* 26:4480–4488. <https://doi.org/10.1021/la903111j>
- Lamaming J, Hashim R, Leh CP et al (2015a) Isolation and characterization of cellulose nanocrystals from parenchyma and vascular bundle of oil palm trunk (*Elaeis guineensis*). *Carbohydr Polym* 134:534–540. <https://doi.org/10.1016/j.carbpol.2015.08.017>
- Lamaming J, Hashim R, Sulaiman O et al (2015b) Cellulose nanocrystals isolated from oil palm trunk. *Carbohydr Polym* 127:202–208. <https://doi.org/10.1016/j.carbpol.2015.03.043>
- Ludueña LN, Vecchio A, Stefani PM, Alvarez VA (2013) Extraction of cellulose nanowhiskers from natural fibers and agricultural byproducts. *Fibers Polym* 14:1118–1127. <https://doi.org/10.1007/s12221-013-1118-z>
- Luzi F, Puglia D, Sarasini F et al (2019) Valorization and extraction of cellulose nanocrystals from North African grass: *Ampelodesmos mauritanicus* (Diss). *Carbohydr Polym* 209:328–337. <https://doi.org/10.1016/j.carbpol.2019.01.048>
- Mendes CADC, Ferreira NMS, Furtado CRG, De Sousa AMF (2015) Isolation and characterization of nanocrystalline cellulose from corn husk. *Mater Lett* 148:26–29. <https://doi.org/10.1016/j.matlet.2015.02.047>
- Meng F, Wang G, Du X et al (2019) Extraction and characterization of cellulose nanofibers and nanocrystals from liquefied banana pseudo-stem residue. *Compos Part B Eng* 160:341–347. <https://doi.org/10.1016/j.compositesb.2018.08.048>
- Mokbli S, Sbihi HM, Nehdi IA et al (2018) Characteristics of *Chamaerops humilis* L. var. *humilis* seed oil and study of the oxidative stability by blending with soybean oil. *J Food Sci Technol* 55:2170–2179. <https://doi.org/10.1007/s13197-018-3134-x>
- Nishiyama Y, Johnson GP, French AD (2012) Diffraction from nonperiodic models of cellulose crystals. *Cellulose* 19:319–336. <https://doi.org/10.1007/s10570-012-9652-1>
- Oun AA, Rhim JW (2016) Characterization of nanocelluloses isolated from Ushar (*Calotropis procera*) seed fiber: effect of isolation method. *Mater Lett* 168:146–150. <https://doi.org/10.1016/j.matlet.2016.01.052>
- Phuong VT, Gigante V, Aliotta L et al (2017) Reactively extruded eco-composites based on poly(lactic acid)/bisphenol A polycarbonate blends reinforced with regenerated cellulose microfibrils. *Compos Sci Technol* 139:127–137. <https://doi.org/10.1016/j.compscitech.2016.12.013>
- Prasad Reddy J, Rhim JW (2014) Isolation and characterization of cellulose nanocrystals from garlic skin. *Mater Lett* 129:20–23. <https://doi.org/10.1016/j.matlet.2014.05.019>
- Rajinipriya M, Nagalakshmaiah M, Robert M, Elkoun S (2018) Importance of agricultural and industrial waste in the field of nanocellulose and recent industrial developments of

- wood based nanocellulose: a review. *ACS Sustain Chem Eng* 6:2807–2828. <https://doi.org/10.1021/acssuschemeng.7b03437>
- Rasheed M, Jawaid M, Parveez B et al (2020) Morphological, chemical and thermal analysis of cellulose nanocrystals extracted from bamboo fibre. *Int J Biol Macromol* 160:183–191. <https://doi.org/10.1016/j.ijbiomac.2020.05.170>
- Sacui IA, Nieuwendaal RC, Burnett DJ et al (2014) Comparison of the properties of cellulose nanocrystals and cellulose nanofibrils isolated from bacteria, tunicate, and wood processed using acid, enzymatic, mechanical, and oxidative methods. *ACS Appl Mater Interfaces* 6:6127–6138. <https://doi.org/10.1021/am500359f>
- Sharma A, Thakur M, Bhattacharya M et al (2019) Commercial application of cellulose nano-composites—a review. *Biotechnol Rep* 21:e00316. <https://doi.org/10.1016/j.btre.2019.e00316>
- Silvério HA, Pires W, Neto F et al (2013) Extraction and characterization of cellulose nanocrystals from corncob for application as reinforcing agent in nanocomposites. *Ind Crops Prod* 44:427–436. <https://doi.org/10.1016/j.indcrop.2012.10.014>
- Wu J, Du X, Yin Z et al (2019) Preparation and characterization of cellulose nanofibrils from coconut coir fibers and their reinforcements in biodegradable composite films. *Carbohydr Polym* 211:49–56. <https://doi.org/10.1016/j.carbpol.2019.01.093>
- Youssef B, Soumia A, Mounir EA et al (2015) Preparation and properties of bionanocomposite films reinforced with nanocellulose isolated from moroccan alfa fibres. *Autex Res J* 15:164–172. <https://doi.org/10.1515/aut-2015-0011>
- Yu HY, Zhang DZ, Lu FF, Yao J (2016) New Approach for single-step extraction of carboxylated cellulose nanocrystals for their use as adsorbents and flocculants. *ACS Sustain Chem Eng* 4:2632–2643. <https://doi.org/10.1021/acssuschemeng.6b00126>

**Publisher's Note** Springer Nature remains neutral with regard to jurisdictional claims in published maps and institutional affiliations.